Stereochemically Rigid Seven-Coordinate Complexes. Synthesis, Structure, and Dynamic Stereochemistry of Chlorotris(*N,N*-dialkylmonothiocarbamato)titanium(IV) Complexes

Stephen L. Hawthorne and Robert C. Fay*

Contribution from the Department of Chemistry, Cornell University, Ithaca, New York 14853.

Received March 5, 1979

Abstract: Seven-coordinate *N,N*-dialkylmonothiocarbamate complexes of the type [Ti(R_2mtc)$_3$Cl] (R_2mtc = $SOCNR_2$; R = Me, Et, *i*-Pr, or *i*-Bu) have been prepared by reaction of titanium(IV) chloride with stoichiometric amounts of Na(R_2mtc) in dichloromethane or benzene. The complexes have been characterized by conductance measurements, NMR spectra, and infrared spectra. The crystal and molecular structure of [Ti(Et_2mtc)$_3$Cl] has been determined by X-ray diffraction and has been refined anisotropically by least-squares methods to $R_1 = 0.062$ and $R_2 = 0.066$ using 4862 independent diffractometer data having $2\theta_{\mathrm{Mo}K\bar{\alpha}} \leq 56.75°$ and $|F_o| \geq 1.58\sigma_F$. The compound crystallizes in the monoclinic space group $C2/c$ with eight molecules in a cell having dimensions $a = 27.888$ (5) Å, $b = 9.786$ (1) Å, $c = 17.819$ (2) Å, $\beta = 97.674$ (9)° ($\rho_{\mathrm{obsd}} = 1.328$, $\rho_{\mathrm{calcd}} = 1.323$ g cm^{-3}). The crystal contains discrete seven-coordinate molecules which have pentagonal bipyramidal geometry and approximate symmetry C_s-*m*. The chlorine atom occupies an axial position (Ti–Cl = 2.330 (1) Å), and the monothiocarbamate ligands are oriented so as to cluster the three sulfur atoms in all-cis positions on one triangular face of the pentagonal bipyramid (Ti–S = 2.477–2.489 Å; Ti–O = 2.076–2.089 Å). Low-temperature ^{1}H NMR spectra of [Ti(Me_2mtc)$_3$Cl] favor the same structure in solution. At higher temperatures, NMR line-shape changes indicate the existence of two distinct kinetic processes: (1) a low-temperature intramolecular metal-centered rearrangement process that exchanges the spanning and the equatorial Me_2mtc ligands ($\Delta G^{\ddagger}$ (−58.2 °C) = 10.8 ± 0.1 kcal/mol, $\Delta H^{\ddagger} = 11.2 \pm 0.3$ kcal/mol, $\Delta S^{\ddagger} = 2.0 \pm 1.6$ eu) and (2) a high-temperature process that involves rotation about the C$\overset{\cdots}{-}$N bond in the Me_2mtc ligands ($\Delta G^{\ddagger}$ (110 °C) = 20 kcal/mol). A polytopal rearrangement mechanism involving a monocapped octahedral transition state that maintains the all-cis arrangement of sulfur atoms is suggested for the metal-centered rearrangement.

Introduction

Previous papers from this laboratory have described the preparation, characterization, and structure of eight-coordinate tetrakis(*N,N*-dialkylmonothiocarbamate) complexes of titanium(IV) and zirconium(IV), [M(R_2mtc)$_4$], **1**.[1-3] These

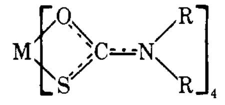

1

complexes exist in the solid state and in solution as dodecahedral stereoisomers which have an *mmmm* ligand wrapping pattern and a C_{2v} arrangement of sulfur and oxygen donor atoms. Two of the sulfur atoms occupy dodecahedral A sites and two occupy B sites so as to give an all-cis arrangement with the four sulfur atoms on one side of the coordination polyhedron and the four oxygen atoms on the other side. These complexes are of special interest as rare examples of eight-coordinate tetrakis chelates that are stereochemically rigid on the NMR time scale at readily accessible temperatures.[4-6]

The present paper reports the preparation and characterization of the seven-coordinate Ti(IV) analogues, [Ti(R_2mtc)$_3$Cl] (R = Me, Et, *i*-Pr, or *i*-Bu), the crystal and molecular structure of [Ti(Et_2mtc)$_3$Cl], and a variable-temperature NMR study of [Ti(Me_2mtc)$_3$Cl]. The seven-coordinate complexes adopt a pentagonal bipyramidal structure that maintains the clustering of sulfur atoms in all-cis positions. [Ti(Me_2mtc)$_3$Cl] becomes rigid on the NMR time scale at temperatures below −58 °C, and to our knowledge this compound is only the second example of a stereochemically rigid seven-coordinate halotris(chelate) complex.[7]

Experimental Section

Reagents and General Techniques. Sodium *N,N*-dimethylmonothiocarbamate, Na(Me_2mtc), and sodium *N,N*-diethylmonothiocarbamate, Na(Et_2mtc), were prepared as previously described.[2] Titanium(IV) chloride (Matheson Coleman and Bell) and carbonyl sulfide (Matheson Gas Products) were used as purchased without further purification. Amines were distilled from sodium immediately before use. Solvents were dried by refluxing over calcium hydride for at least 24 h and were distilled immediately before use. All syntheses and subsequent handling of the compounds were conducted under anhydrous conditions in a dry nitrogen atmosphere.

Sodium *N,N*-Diisopropylmonothiocarbamate, Na(*i*-Pr_2mtc). With stirring at 0 °C, carbonyl sulfide was bubbled very slowly for 24 h through a mixture of diisopropylamine (66.2 mL, 469 mmol) and sodium hydride (4.94 g, 206 mmol) in acetonitrile (280 mL). The pale yellow solution was filtered, and solvent was pumped off until the volume was ~90 mL. Addition of benzene (400 mL) afforded a white precipitate which was filtered, washed with three 50-mL portions of benzene, and dried in vacuo for 20 h, yield 20.17 g (53%), mp 228–231 °C dec. Anal. Calcd for Na(C_7H_{14}NOS): C, 45.88; H, 7.70; N, 7.64; Na, 12.55. Found: C, 45.68; H, 8.06; N, 7.49; Na, 12.23.

Sodium *N,N*-Diisobutylmonothiocarbamate, Na(*i*-Bu_2mtc). With stirring at 0 °C, carbonyl sulfide was bubbled slowly for 2.5 h through a mixture of diisobutylamine (75 mL, 410 mmol) and sodium hydride (3.47 g, 145 mmol) in benzene (250 mL). The mixture was stirred at room temperature for 18 h and then warmed gradually until it refluxed; since the reaction rate increased dramatically with the rise in temperature, the warming process was accomplished over a period of 5 days to avoid excessive foaming. After the solution had refluxed for 2 days, the insoluble white product was filtered, washed with two 50-mL portions of benzene, and dried in vacuo for 27 h, yield 25.23 g (83%), mp 210–212 °C. Anal. Calcd for Na(C_9H_{18}NOS): C, 51.16; H, 8.59; N, 6.63; Na, 10.88. Found: C, 50.89; H, 8.66; N, 6.57; Na, 10.70.

Chlorotris(*N,N*-dimethylmonothiocarbamato)titanium(IV), [Ti(Me_2mtc)$_3$Cl]. Titanium(IV) chloride (1.18 mL, 10.7 mmol) was added with rapid stirring to a suspension of Na(Me_2mtc) (4.10 g, 32.2 mmol) in dichloromethane (150 mL), and the mixture was allowed to reflux for 5 h. The mixture was then filtered and the sodium chloride precipitate washed with three 15-mL portions of dichloromethane. Reduction of the combined filtrate and washings to ~70 mL followed by addition of ~150 mL of hexane afforded an orange powder, which was dried in vacuo at 100 °C for 24 h to remove dichloromethane of crystallization, yield 3.35 g (79%), mp 188–200 °C dec. Anal. Calcd

0002-7863/79/1501-5268$01.00/0

for $Ti(C_3H_6NOS)_3Cl$: C, 27.31; H, 4.58; Cl, 8.96; N, 10.62; Ti, 12.10. Found: C, 27.10; H, 4.68; Cl, 9.07; N, 10.55; Ti, 12.24.

Chlorotris(*N,N*-diethylmonothiocarbamato)titanium(IV), [Ti(Et$_2$mtc)$_3$Cl]. This complex was prepared from titanium(IV) chloride (3.15 mL, 28.7 mmol) and Na(Et$_2$mtc) (13.40 g, 86.3 mmol) in dichloromethane (125 mL) using a procedure similar to that employed for preparation of [Ti(Me$_2$mtc)$_3$Cl]. The yield of large, red crystals was 11.14 g (81%), mp 129–149 °C dec. Anal. Calcd for $Ti(C_5H_{10}NOS)_3Cl$: C, 37.54; H, 6.30; Cl, 7.39; N, 8.75; S, 20.04; Ti, 9.98. Found: C, 37.48; H, 6.27; Cl, 7.60; N, 8.71; S, 19.90; Ti, 10.02.

Chlorotris(*N,N*-diisopropylmonothiocarbamato)titanium(IV), [Ti(*i*-Pr$_2$mtc)$_3$Cl]. This complex was prepared in 72% yield by reaction of titanium(IV) chloride (0.40 mL, 3.6 mmol) with Na(*i*-Pr$_2$mtc) (2.00 g, 10.9 mmol) in dichloromethane (125 mL). The resulting orange powder was dried in vacuo at 100 °C for 13.5 h to remove dichloromethane of crystallization, mp 153–156 °C. Anal. Calcd for $Ti(C_7H_{14}NOS)_3Cl$: C, 44.71; H, 7.50; Cl, 6.28; N, 7.45; Ti, 8.49. Found: C, 44.86; H, 7.63; Cl, 6.57; N, 7.32; Ti, 8.70.

Chlorotris(*N,N*-diisobutylmonothiocarbamato)titanium(IV), [Ti(*i*-Bu$_2$mtc)$_3$Cl]. This complex was prepared from titanium(IV) chloride (1.30 mL, 11.8 mmol) and Na(*i*-Bu$_2$mtc) (7.73 g, 36.6 mmol) in benzene (170 mL). The resulting bright yellow powder was dried in vacuo at 100 °C over 18 h to remove benzene of crystallization, yield 5.60 g (73%), mp 168–171 °C. Anal. Calcd for $Ti(C_9H_{18}NOS)_3Cl$: C, 50.02; H, 8.40; Cl, 5.47; N, 6.48; Ti, 7.39. Found: C, 50.13; H, 8.52; Cl, 5.61; N, 6.55; Ti, 7.27.

Bromotris(*N,N*-dimethylmonothiocarbamato)titanium(IV), [Ti(Me$_2$mtc)$_3$Br]. This complex was prepared in 55% yield by reaction of Na(Me$_2$mtc) (2.28 g, 15.9 mmol) with titanium(IV) bromide (2.20 g, 5.99 mmol) in refluxing dichloromethane (125 mL). Crystallization of the crude product from dichloromethane-hexane (1:2 v/v) afforded large, red crystals which were dried in vacuo at 60 °C for 12 h to remove dichloromethane of crystallization, mp 158–175 °C dec. Anal. Calcd for $Ti(C_3H_6NOS)_3Br$: C, 24.55; H, 4.12; Br, 18.15; N, 9.54; Ti, 10.88. Found: C, 24.30; H, 4.37; Br, 18.30; N, 9.72; Ti, 11.07.

Conductance Measurements. Conductance measurements were made in dichloromethane at 25.00 ± 0.05 °C with an Industrial Instruments Model RC 16B2 conductivity bridge and a Freas-type solution cell with bright platinum electrodes. The bridge frequency was 60 Hz, and the cell constant was 0.113 cm^{-1}. The specific conductance of the purified solvent was less than $4.5 \times 10^{-8}\ \Omega^{-1}\ cm^{-1}$.

Infrared Spectra. Infrared spectra were recorded in the region 4000-250 cm^{-1} with a Perkin-Elmer 521 grating spectrophotometer. The complexes were studied as mineral oil mulls supported between cesium iodide plates. The estimated uncertainty in reported frequencies is ±4 cm^{-1}.

Nuclear Magnetic Resonance Spectra. Proton chemical shifts and coupling constants were measured at ambient probe temperature (~34 °C) with a Varian EM-390 90-MHz spectrometer. Reported values are the averages of those obtained from at least three sweeps of each spectrum; the sweep width was calibrated with a sample of chloroform and tetramethylsilane.

Variable-temperature pulsed Fourier-transform ^{1}H NMR spectra of a 0.0590 M solution of [Ti(Me$_2$mtc)$_3$Cl] in dichloromethane-d_2 were recorded in the temperature range −86.2 to 49.0 °C with a Bruker HX-90 spectrometer which was locked on the solvent deuterium resonance. Temperatures, determined with a copper-constantan thermocouple immersed in acetone, are estimated to be accurate to ±0.5 °C. Variable-temperature continuous-wave ^{1}H NMR spectra of a 0.0441 M solution of [Ti(Me$_2$mtc)$_3$Cl] in diphenylmethane were recorded in triplicate in the temperature range 39.2–135.0 °C with a Varian EM-390 spectrometer locked on the methylene proton resonance of the solvent. Temperatures, estimated to be accurate to ±0.5 °C, were determined from the temperature-dependent chemical shift between the nonequivalent protons of 1,2-ethanediol.[20] In the recording of both sets of variable-temperature spectra, care was taken to minimize the common sources of error in NMR line-broadening studies,[21] as previously described.[22]

Spectra were analyzed using the line-shape program PZDMFX obtained from P. Meakin of E. I. du Pont de Nemours, Inc. Calculated spectra were evaluated by qualitative comparison with observed spectra, overlaying one on the other, and, in some cases, by comparison of measured parameters (peak separations, relative heights of maxima and minima, and peak widths at one-fourth, one-half, and three-fourths maximum amplitude). The temperature-dependent transverse relaxation times, T_2, used to generate calculated spectra were determined from variable-temperature spectra of *S*-methyl-*N,N*-dimethylmonothiocarbamate, which evidences line broadening due to increasing solvent viscosity, but no line broadening due to kinetic exchange; $\mathrm{C}\overset{\cdots}{-}\mathrm{N}$ bond rotation in Me$_2$NC(O)SMe is fast on the NMR time scale,[23] even at −90 °C.[24]

Crystallography. Several air-sensitive red crystals of [Ti(Et$_2$mtc)$_3$Cl], obtained by recrystallization from dichloromethane-hexane (~1:4 v/v), were sealed under dry nitrogen in 0.3-mm Lindemann capillaries. The lattice symmetry and the systematic extinctions (hkl for $h + k \neq 2n$ and $h0l$ for $l \neq 2n$) observed in precession photographs indicated that the crystals were monoclinic with probable space group $C2/c$ (C_{2h}^6, No. 15).[25] The choice of the centric space group was confirmed by the distribution of reflection intensities[26] and the successful refinement of the structure in that group. The lattice constants of a = 27.888 (5) Å, b = 9.786 (1) Å, c = 17.819 (2) Å, and β = 97.674 (9)° were determined by least-squares refinement of the diffraction geometry for 35 high-angle reflections ($2\theta > 30°$) centered on a computer-controlled, four-circle Picker FACS-I diffractometer using Zr-filtered Mo K$\bar{\alpha}$ radiation (λ = 0.710 69 Å). The density calculated on the basis of eight molecules of [Ti(SOCN(C$_2$H$_5$)$_2$)$_3$Cl] per unit cell is 1.323 g cm^{-3}, which compares favorably with the observed value of 1.328 g cm^{-3} determined by flotation in carbon tetrachloride-hexane.

An irregularly shaped crystal of approximate dimensions 0.25 × 0.35 × 0.60 mm was chosen for collection of intensity data. The data were collected at ambient temperature on the Picker diffractometer employing Zr-filtered Mo K$\bar{\alpha}$ radiation and a takeoff angle of ~3°. Intensities were measured using the θ–2θ scan technique at a scan rate of 1°/min with a scan angle of 2° plus an allowance for dispersion of Mo Kα_1 and Mo Kα_2 radiation. Background counts of 40-s duration were taken at each end of the scan. Reflections having counting rates greater than 10 000 counts/s were automatically attenuated by insertion of copper foil into the path of the diffracted beam until the intensity was reduced to less than that value. The intensities of three standard reflections, monitored at 50-reflection intervals, showed no trend with time. A total of 5686 independent reflections having $2\theta \leq 56.75°$ was collected; these data were corrected for background, use of attenuators, and Lorentz and polarization factors. Since the linear absorption coefficient for Mo K$\bar{\alpha}$ radiation is 7.46 cm^{-1} and the estimated maximum error resulting from neglect of absorption corrections is <7% in any intensity and <4% in any amplitude for the crystal used, absorption corrections were judged unnecessary. Those reflections having $|F_o| < 1.58\sigma_F$, where σ_F is defined elsewhere,[27] were considered "unobserved"; the remaining 4862 reflections were retained for the structure analysis.

Structure Determination and Refinement. The structure was solved by straightforward application of the heavy-atom technique. Analysis of a Patterson synthesis revealed the positions of the titanium and chlorine atoms. With the exception of one of the methyl carbon atoms, the remaining nonhydrogen atoms were located in subsequent Fourier syntheses.

Using the reflections having $0 \leq 2\theta \leq 44.65°$, several cycles of full-matrix least-squares refinement of the positional and thermal parameters of the 25 atoms found in the Fourier syntheses, followed by a difference Fourier synthesis, revealed the location of the remaining carbon atom. This atom was found to be disordered, occupying two sites in approximately equal proportions, as indicated by the peak intensities in the Fourier map; the site-occupancy factors of 0.5 for each site were not refined in subsequent calculations. After several additional cycles of least-squares refinement, a difference Fourier synthesis revealed the positions of all hydrogen atoms except those in the disordered ethyl group. Each hydrogen was assigned an isotropic thermal parameter slightly larger than the isotropic thermal parameter of the carbon to which it was attached. Hydrogen atoms were included in subsequent least-squares calculations but were not refined.

In the final several cycles of refinement, based upon all observed data, all nonhydrogen atoms were refined using anisotropic thermal parameters. Owing to the limited capacity of the full-matrix least-squares computer program used, positional and/or thermal parameters of some atoms were held fixed, a different group of parameters being fixed in each cycle. In the final cycle, positional parameters for all atoms were refined, while all thermal parameters were held constant.

The quantity minimized in the least-squares calculations was $\sum w(|F_o| - |F_c|)^2$. Upon convergence, the residuals

Table I. Proton Chemical Shift[a] and Coupling Constant[b] Data

compd	$>$CH	-CH$_2$-	-CH$_3$	J
Na(i-Pr$_2$mtc)[c]	−5.48, −3.26		−1.11	d
Na(i-Bu$_2$mtc)[c]	−2.04	−3.32	−0.79	6.7, 7.1[e]
[Ti(Me$_2$mtc)$_3$Cl]			−3.19, −3.10	
[Ti(Et$_2$mtc)$_3$Cl]		−3.62, −3.51	−1.21, −1.19	7.2, 7.2[f]
[Ti(i-Pr$_2$mtc)$_3$Cl]	−4.47, −3.65		−1.49, −1.20	6.7, 6.7[f]
[Ti(i-Bu$_2$mtc)$_3$Cl]	−2.06	−3.41, −3.26	−0.89	6.6, 7.7, 7.4[g]
[Ti(Me$_2$mtc)$_3$Br]			−3.22, −3.12	

[a] In parts per million (±0.01) relative to an internal reference of tetramethylsilane (1% by volume) at 34 °C in CDCl$_3$, except as noted. [b] In hertz (±0.2) at 34 °C in CDCl$_3$, except as noted. [c] In dimethyl-d_6 sulfoxide. [d] $J \sim$ 6–7 Hz but resonances are too broad to determine J accurately. [e] The first coupling constant given is J(CH$_3$-CH); the second is J(CH$_2$-CH). [f] The first coupling constant is that involving the downfield methyl resonance; the second is that involving the upfield methyl resonance. [g] The coupling constants are given in the order J(CH$_3$-CH), J(CH$_2$-CH) for downfield methylene resonance and J(CH$_2$-CH) for upfield methylene resonance.

Table II. Characteristic Infrared Frequencies (cm^{-1})[a]

compd	$\nu(\mathrm{C}\overset{\cdots}{-}\mathrm{O})$, $\nu(\mathrm{C}\overset{\cdots}{-}\mathrm{N})$	$\nu(\mathrm{C}\overset{\cdots}{-}\mathrm{S})$	ν(Ti-O)	ν(Ti-S)	ν(Ti-X)	other bands[b]
Na(i-Pr$_2$mtc)	1550 m, 1532 m, 1509 s	920 m				1419 m, 1287 vs, 1213 m, 1164 w, 1148 m, 1134 m, 1115 m, 1038 s, 944 w, 876 m, 831 m, 800 s, 691 m, 634 m, 524 m, 471 m, 424 w, 395 m, 358 w, 295 m
Na(i-Bu$_2$mtc)	1497 s	918 m				1437 s, 1422 m, 1400 m, 1355 w, 1336 m, 1302 w, 1286 m, 1226 s, 1172 w, 1146 s, 1131 w, 1115 sh, 1095 m, 988 m, 957 w, 942 m, 894 w, 878 w, 864 w, 812 m, 734 m, 694 m, 592 w, 555 w, 516 w, 454 w, 438 w, 402 w, 371 vw, 331 w, 287 w
[Ti(Me$_2$mtc)$_3$Cl]	1572 s,b	930 m	550 s	318 m	361 s	1420 w, 1401 m, 1367 m, 1313 w, 1244 m, 1134 s, 1054 w, 705 m, 658 m, 481 m, 404 m
[Ti(Et$_2$mtc)$_3$Cl]	1548 s,b	945 m	554 s	316 w	347 s	1443 m, 1313 w, 1300 w, 1265 s, 1210 m, 1140 s, 1100 w, 1080 m, 1073 w, 1020 vw, 887 s, 787 w, 683 s, 671 s, 523 w, 471 w, 458 w, 398 m, 290 w, 268 w
[Ti(i-Pr$_2$mtc)$_3$Cl]	1531 s,b	925 m	572 s	331 m	352 m	1401 w, 1357 w, 1345 w, 1306 s, 1207 m, 1168 w, 1151 m, 1124 w, 1040 s, 881 m, 841 m, 766 w, 674 m, 640 m, 540 w, 526 m, 421 w, 393 m, 383 w
[Ti(i-Bu$_2$mtc)$_3$Cl]	1530 s,b	923 w	558 s	324 m	366 s	1340 m, 1286 m, 1243 s, 1199 m, 1172 w, 1143 s, 1122 w, 1104 w, 1024 w, 948 w, 892 w, 817 m, 746 s, 668 m, 497 w, 484 m, 402 m
[Ti(Me$_2$mtc)$_3$Br]	1571 s,b	930 m	547 s	319 s,b	319 s,b	1416 w, 1400 m, 1366 m, 1308 w, 1242 m, 1131 s, 1051 w, 701 s, 654 m, 479 m, 402 s, 352 w

[a] As Nujol oil mulls between CsI plates. [b] 2000–250-cm^{-1} region.

$$R_1 = \sum||F_o| - |F_c||/\sum|F_o|$$

and

$$R_2 = [\sum w(|F_o| - |F_c|)^2/\sum w|F_o|^2]^{1/2}$$

were 0.062 and 0.066, respectively. Unit weighting was used throughout the refinement. In the last cycle of refinement no coordinate shifted by more than 0.03σ, the average shift being 0.01σ. A final difference Fourier showed no anomalous features; most of the larger peaks were located in the vicinity of the disordered ethyl group, the largest being 0.45 e/Å^3.

Scattering factors were taken from Cromer and Mann[28] for Ti^0, Cl^0, S^0, O^0, N^0, and C^0 and from Stewart, Davidson, and Simpson[29] for H^0. Anomalous dispersion corrections, real and imaginary, for Ti, S, and Cl were obtained from Cromer.[30] Calculations were carried out on PRIME 300 and IBM 370/168 computers using programs listed in a previous paper.[3]

Results and Discussion

Preparation and Properties. Titanium(IV) N,N-dialkylmonothiocarbamates of the type [Ti(R$_2$mtc)$_3$Cl] (R = Me, Et, i-Pr, i-Bu) have been prepared in good yield by reaction of titanium(IV) chloride with stoichiometric amounts of sodium N,N-dialkylmonothiocarbamates in dichloromethane or benzene:

$$\mathrm{TiCl_4 + 3Na(SOCNR_2) \rightarrow [Ti(SOCNR_2)_3Cl] + 3NaCl} \quad (1)$$

[Ti(Me$_2$mtc)$_3$Br] was synthesized by an analogous procedure. The intermediate sodium salts were prepared by a previously described method.[2] The methods used for preparation and isolation of these compounds (see Experimental Section) give

Table III. Final Atomic Fractional Coordinates for $[Ti(Et_2mtc)_3Cl]$[a]

atom	10^4x	10^4y	10^4z
Ti	3614.6 (3)	4956.6 (7)	1015.6 (4)
Cl	4170.9 (4)	6574 (1)	1551.4 (6)
S_a	3118.4 (5)	2896 (1)	669.5 (7)
S_b	2868.5 (4)	6358 (1)	829.5 (6)
S_c	3563.3 (4)	5758 (1)	−318.5 (6)
O_a	3874 (1)	3240 (3)	1638 (2)
O_b	3299 (1)	5203 (3)	1999 (1)
O_c	4153 (1)	4169 (3)	441 (2)
N_a	3735 (2)	1002 (4)	1360 (3)
N_b	2722 (1)	6667 (4)	2288 (2)
N_c	4343 (1)	4444 (4)	−746 (2)
C_a	3616 (2)	2322 (4)	1273 (2)
C_b	2964 (2)	6058 (4)	1792 (2)
C_c	4066 (2)	4702 (4)	−218 (2)
C_{a1}	3437 (3)	−85 (5)	947 (4)
C_{a2}	3574 (3)	−416 (6)	185 (4)
C_{a3}	4214 (3)	630 (6)	1810 (4)
C_{a4a}	4231 (5)	133 (14)	2534 (7)
C_{a4b}	4584 (5)	684 (24)	1460 (11)
C_{b1}	2306 (2)	7581 (6)	2050 (3)
C_{b2}	1838 (2)	6817 (8)	1958 (4)
C_{b3}	2868 (2)	6457 (5)	3110 (3)
C_{b4}	3194 (3)	7585 (7)	3451 (4)
C_{c1}	4254 (2)	5050 (7)	−1512 (3)
C_{c2}	4590 (3)	6170 (9)	−1619 (4)
C_{c3}	4757 (2)	3508 (6)	−571 (3)
C_{c4}	4638 (3)	2062 (9)	−785 (6)

[a] The figure in parentheses following each datum is the estimated standard deviation in the last significant figure.

products of good purity as judged by satisfactory elemental analyses and by ^1H NMR spectra (Table I).

The $[Ti(R_2mtc)_3Cl]$ complexes are soluble in dichloromethane and chloroform, less soluble in benzene, and essentially insoluble in saturated hydrocarbons; solubility increases with increasing size of the alkyl group. The complexes are thermally stable, but they are hydrolyzed rapidly upon exposure to air, showing evidence of hydrolysis within minutes in the solid state, and almost instantaneously in solution. Qualitative observations indicate that the hydrolysis rate increases with decreasing size of the alkyl substituent. Conductance measurements show that all of the $[Ti(R_2mtc)_3Cl]$ complexes behave as nonelectrolytes in dichloromethane solution; molar conductances of 10^{-3} M solutions are $\leq 0.39\ \Omega^{-1}\ cm^2\ mol^{-1}$.

Infrared frequencies are listed in Table II. Except for the Ti–Cl stretching vibrations at 347–366 cm^{-1}, the infrared spectra of the $[Ti(R_2mtc)_3Cl]$ complexes are very similar to spectra of the corresponding $[Ti(R_2mtc)_4]$ complexes,[2] exhibiting an intense, broad band in the region 1530–1572 cm^{-1} due to coupled $\nu(C\overset{...}{-}O)$ and $\nu(C\overset{...}{-}N)$ stretching vibrations,[31] a $\nu C\overset{...}{-}S)$ stretching frequency at 923–945 cm^{-1}, ν(Ti–O) at 550–572 cm^{-1}, and ν(Ti–S) at 316–331 cm^{-1}. Comparison of these frequencies with frequencies of the corresponding bands for the eight-coordinate $[Ti(R_2mtc)_4]$ complexes[2] reveals no systematic dependence on coordination number, except that the band due to coupled $\nu(C\overset{...}{-}O)$ and $\nu(C\overset{...}{-}N)$ stretching vibrations occurs at higher frequencies (by ~15–30 cm^{-1}) in the seven-coordinate $[Ti(R_2mtc)_3Cl]$ complexes. A similar trend has been noted for the analogous Ti(IV) dithiocarbamates.[10] In $[Ti(Me_2mtc)_3Br]$, the ν(Ti–Br) and ν(Ti–S) bands give rise to a strong, broad band at 319 cm^{-1}, and the 347–366 cm^{-1} ν(Ti–Cl) band is not observed.

Solid-State Structure of $[Ti(Et_2mtc)_3Cl]$. In order to establish the coordination geometry of a representative $[Ti(R_2mtc)_3Cl]$ complex in the solid state, the structure of $[Ti(Et_2mtc)_3Cl]$ was determined by X-ray diffraction. Final atomic coordinates and thermal parameters are presented in Tables III and IV, re-

Table IV. Final Thermal Parameters for $[Ti(Et_2mtc)_3Cl]$[a] ($Å^2$)

atom	anisotropic parameters						equivalent isotropic
	B_{11}[b]	B_{22}	B_{33}	B_{12}	B_{13}	B_{23}	B[c]
Ti	3.09 (3)	2.16 (3)	2.36 (3)	0.41 (2)	0.82 (2)	0.12 (2)	2.42 (2)
Cl	4.13 (5)	3.41 (5)	3.83 (5)	−0.63 (4)	0.96 (4)	−0.57 (4)	3.67 (3)
S_a	4.00 (5)	3.25 (5)	4.17 (5)	−0.45 (4)	0.55 (4)	−0.02 (4)	3.77 (3)
S_b	4.02 (5)	4.02 (5)	3.03 (4)	1.38 (4)	0.91 (4)	0.59 (4)	3.44 (3)
S_c	4.42 (6)	3.90 (5)	2.63 (4)	1.05 (4)	0.95 (4)	0.45 (4)	3.41 (3)
O_a	4.2 (1)	2.5 (1)	2.8 (1)	0.5 (1)	0.6 (1)	0.2 (1)	3.04 (8)
O_b	3.4 (1)	2.9 (1)	2.6 (1)	1.0 (1)	1.2 (1)	0.4 (1)	2.70 (8)
O_c	3.6 (1)	3.3 (1)	2.8 (1)	0.8 (1)	1.2 (1)	0.3 (1)	3.05 (8)
N_a	7.4 (3)	2.0 (1)	4.9 (2)	0.4 (2)	0.5 (2)	0.0 (1)	4.2 (1)
N_b	4.4 (2)	3.2 (2)	3.5 (2)	1.4 (1)	1.6 (1)	0.1 (1)	3.3 (1)
N_c	3.3 (2)	4.6 (2)	2.9 (1)	0.1 (1)	1.0 (1)	−0.5 (1)	3.4 (1)
C_a	5.0 (2)	2.2 (2)	2.9 (2)	0.1 (2)	1.3 (2)	0.3 (1)	3.1 (1)
C_b	3.4 (2)	2.6 (2)	2.9 (2)	0.3 (1)	1.2 (1)	0.0 (1)	2.8 (1)
C_c	3.5 (2)	2.7 (2)	2.7 (2)	0.0 (1)	1.0 (1)	−0.5 (1)	2.8 (1)
C_{a1}	9.7 (5)	2.3 (2)	6.3 (3)	−1.0 (2)	0.4 (3)	0.1 (2)	5.2 (2)
C_{a2}	12.2 (6)	3.5 (3)	5.4 (3)	0.0 (3)	1.8 (3)	−1.4 (2)	5.9 (2)
C_{a3}	11.1 (6)	2.7 (2)	8.4 (4)	1.9 (3)	−3.2 (4)	0.1 (3)	5.8 (3)
C_{a4a}	7.1 (7)	6.0 (7)	5.7 (6)	0.8 (6)	0.8 (5)	2.7 (5)	5.8 (5)
C_{a4b}	4.5 (7)	15 (2)	11 (1)	1.8 (9)	1.5 (7)	−2 (1)	8.8 (8)
C_{b1}	6.1 (3)	4.4 (2)	4.7 (2)	3.0 (2)	2.1 (2)	0.8 (2)	4.2 (2)
C_{b2}	4.8 (3)	8.1 (4)	5.8 (3)	2.5 (3)	1.8 (2)	1.9 (3)	5.5 (2)
C_{b3}	5.7 (3)	3.8 (2)	3.3 (2)	1.2 (2)	2.0 (2)	0.0 (2)	3.7 (2)
C_{b4}	10.3 (5)	5.6 (3)	5.6 (3)	−0.5 (3)	−1.1 (3)	−0.4 (3)	6.8 (2)
C_{c1}	5.3 (3)	7.2 (3)	2.6 (2)	−0.1 (3)	1.4 (2)	−0.4 (2)	4.4 (2)
C_{c2}	7.4 (4)	11.4 (6)	5.2 (3)	−3.2 (4)	0.2 (3)	3.2 (4)	6.7 (3)
C_{c3}	4.0 (2)	5.9 (3)	4.6 (2)	0.7 (2)	1.9 (2)	−0.7 (2)	4.4 (2)
C_{c4}	8.4 (5)	6.2 (4)	16.2 (8)	2.5 (4)	0.5 (5)	−3.0 (5)	8.7 (4)

[a] The figure in parentheses following each datum is the estimated standard deviation in the last significant figure. [b] Anisotropic temperature factors are of the form $\exp[-(\beta_{11}h^2 + \beta_{22}k^2 + \beta_{33}l^2 + 2\beta_{12}hk + 2\beta_{13}hl + 2\beta_{23}kl)]$; the B_{ij} in $Å^2$ are related to the dimensionless β_{ij} employed during refinement as $B_{ij} = 4\beta/a_i^*a_j^*$. [c] Isotropic thermal parameter calculated from $B = 4[V^2 \det(\beta_{ij})]^{1/3}$.

Table V. Final Parameters for the Hydrogen Atoms of [Ti(Et$_2$mtc)$_3$Cl]

atom[a]	10^3x	10^3y	10^3z	B,[b] Å^2	distance, Å
H_1 (a1)	339	−88	135	7.0	1.07
H_2 (a1)	313	20	78	7.0	0.91
H_3 (a2)	400	−60	27	7.5	1.18
H_4 (a2)	361	46	−23	7.5	1.15
H_5 (a2)	358	−122	−3	7.5	0.87
H_6 (b1)	236	815	158	5.5	1.03
H_7 (b1)	227	823	243	5.5	0.95
H_8 (b2)	179	619	144	7.0	1.10
H_9 (b2)	181	617	236	7.0	0.96
H_{10} (b2)	161	746	191	7.0	0.90
H_{11} (b3)	257	653	339	5.0	1.03
H_{12} (b3)	304	551	317	5.0	1.05
H_{13} (b4)	352	755	318	7.5	1.09
H_{14} (b4)	336	749	385	7.5	0.81
H_{15} (b4)	304	823	341	7.5	0.76
H_{16} (c1)	391	546	−156	5.5	1.03
H_{17} (c1)	428	431	−183	5.5	0.93
H_{18} (c2)	457	635	−217	7.5	0.99
H_{19} (c2)	481	633	−141	7.5	0.70
H_{20} (c2)	456	692	−123	7.5	1.02
H_{21} (c3)	502	384	−85	5.5	0.99
H_{22} (c3)	490	368	0	5.5	1.05
H_{23} (c4)	438	187	−50	11.0	0.95
H_{24} (c4)	497	124	−48	11.0	1.28
H_{25} (c4)	456	223	−137	11.0	1.05

[a] Symbol in parentheses designates the carbon atom to which the hydrogen is bonded at a distance given in the last column. The hydrogen atoms bonded to carbon atoms C_{a3}, C_{a4a}, and C_{a4b} were not located. [b] Assigned at a value slightly larger than the isotropic thermal parameter of the carbon atom to which the hydrogen is bonded.

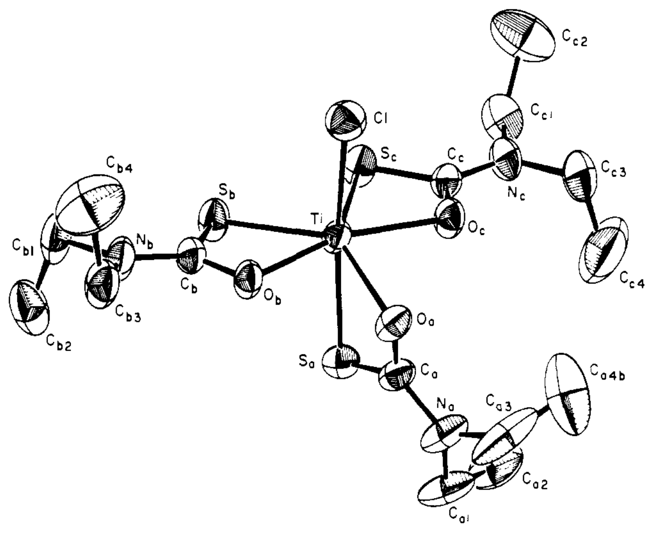

Figure 1. Model in perspective of the [Ti(Et$_2$mtc)$_3$Cl] molecule. Each atom is represented by a 50%-probability thermal ellipsoid consistent with the thermal parameters in Table IV. One of the two positions occupied by the disordered carbon atom C_{a4} has been omitted for clarity.

Table VI. Bond Distances, Polyhedral Edge Lengths, and Bond Angles in the Coordination Group of [Ti(Et$_2$mtc)$_3$Cl][a]

atoms	length, Å	atoms	angle, deg
Ti-Cl	2.330 (1)	Cl-Ti-S$_a$	167.05 (5)
Ti-S$_a$	2.477 (2)		
Ti-S$_b$	2.477 (2)		
Ti-S$_c$	2.489 (1)		
Ti-O$_a$	2.089 (3)		
Ti-O$_b$	2.078 (3)		
Ti-O$_c$	2.076 (3)		
Cl···S$_b$	3.694 (2)	Cl-Ti-S$_b$	100.38 (5)
Cl···S$_c$	3.620 (2)	Cl-Ti-S$_c$	97.32 (5)
Cl···O$_a$	3.375 (3)	Cl-Ti-O$_a$	99.45 (9)
Cl···O$_b$	2.978 (3)	Cl-Ti-O$_b$	84.81 (9)
Cl···O$_c$	3.071 (3)	Cl-Ti-O$_c$	88.20 (10)
S$_a$···S$_b$	3.478 (2)	S$_a$-Ti-S$_b$	89.19 (5)
S$_a$···S$_c$	3.615 (2)	S$_a$-Ti-S$_c$	93.43 (5)
S$_a$···O$_a$[b]	2.562 (3)	S$_a$-Ti-O$_a$	67.66 (9)
S$_a$···O$_b$	3.262 (3)	S$_a$-Ti-O$_b$	91.08 (9)
S$_a$···O$_c$	3.219 (4)	S$_a$-Ti-O$_c$	89.53 (10)
S$_b$···S$_c$	3.057 (2)	S$_b$-Ti-S$_c$	75.97 (4)
S$_b$···O$_b$[b]	2.529 (3)	S$_b$-Ti-O$_b$	66.78 (8)
S$_c$···O$_c$[b]	2.522 (3)	S$_c$-Ti-O$_c$	66.35 (9)
O$_a$···O$_b$	2.637 (4)	O$_a$-Ti-O$_b$	78.54 (11)
O$_a$···O$_c$	2.535 (4)	O$_a$-Ti-O$_c$	74.99 (11)

[a] Numbers in parentheses are estimated standard deviations in the last significant figure. [b] The "bite" of the ligand.

spectively; hydrogen atom parameters are given in Table V. A table of observed and calculated structure factor amplitudes is available.[32] A perspective view of the molecule showing the atom numbering scheme is presented in Figure 1; atoms of the three *N,N*-diethylmonothiocarbamate ligands are distinguished by a literal subscript (a, b, or c). Bond distances, polyhedral edge lengths, and bond angles in the coordination group are given in Table VI.

The [Ti(Et$_2$mtc)$_3$Cl] complex is seven coordinate, adopting a somewhat distorted pentagonal bipyramidal structure which resembles that of chlorotris(*N,N*-dimethyldithiocarbamato)titanium(IV), [Ti(Me$_2$dtc)$_3$Cl].[33] The chlorine atom occupies an axial position; monothiocarbamate ligand a spans the other axial position and one equatorial position, while monothiocarbamate ligands b and c are located in the remaining equatorial positions. The unsymmetrical bidentate ligands are oriented in such a way as to cluster the three sulfur atoms in all-cis positions on one triangular face of the pentagonal bipyramid (Figure 1). Neglecting the methyl carbon atoms of the monothiocarbamate ligands, the maximum permissible symmetry for this configuration, C_s-m, is closely approximated, with the atoms Ti, Cl, S$_a$, and O$_a$ lying in the quasi-mirror plane, and bidentate ligands b and c being symmetrically disposed about this plane. The structures of $[Ti(Et_2mtc)_3Cl]$ and the eight-coordinate analogue, $[Ti(Et_2mtc)_4]$,[3] are closely related in that both exhibit an all-cis arrangement of sulfur atoms. Conceptually, the pentagonal bipyramidal structure of $[Ti(Et_2mtc)_3Cl]$ can be generated from the dodecahedral structure of $[Ti(Et_2mtc)_4]$ simply by replacing with a chlorine atom one of the two monothiocarbamate ligands that has an oxygen atom in an A site and a sulfur atom in a B site.

The principal distortions from idealized pentagonal bipyramidal geometry in $[Ti(Et_2mtc)_3Cl]$, similar to those observed for $[Ti(Me_2dtc)_3Cl]$, can be seen in Figure 2, which is a projection of the TiS_3O_3Cl coordination group onto the quasi-mirror plane containing the atoms Ti, Cl, S_a, and O_a; the mean displacement of these four atoms from the quasi-mirror plane is 0.011 Å (cf. Table VIII[32]). The atoms Ti, S_b, S_c, O_b, and O_c are coplanar to within 0.08 Å (cf. Table VIII[32]); this equatorial plane is very nearly perpendicular to the quasi-mirror plane, the dihedral angle being 89.9° (90° for an idealized pentagonal bipyramid). The $Ti-S_a$ bond is located very close to the quasi-fivefold axis (1.2° off), but oxygen atom O_a is well below the equatorial plane (0.77 Å), since the 2.5-2.6-Å "bite" of the monothiocarbamate ligand does not allow it to span a 90° angle. The Ti-Cl bond is located 11.7° off the quasi-fivefold axis; this distortion is probably related to the positioning of O_a below the equatorial plane, which allows the Cl atom to move in the direction of O_a, thus relieving nonbonded repulsions between itself and S_b and S_c.

Values of the δ shape parameters[34] for the TiS_3O_3Cl coordination polyhedron in $[Ti(Et_2mtc)_3Cl]$ are 40.8, 42.3, and −60.4°. These are the dihedral angles between the polyhedral faces which intersect along the edges $S_a \cdots O_b$, $S_a \cdots O_c$, and $O_b \cdots O_c$, respectively; the third δ value is negative because the edge $O_b \cdots O_c$ is not an exterior polyhedral edge. In view of the constraints imposed upon the coordination geometry by the presence of inequivalent donor atoms and chelating ligands, the δ values for the complex are in reasonable agreement with those calculated for an idealized D_{5h} pentagonal bipyramid (54.4, 54.4, and −72.8°). The observed δ values differ substantially from those expected for the C_{3v} monocapped octahedron (16.2, 16.2, and 16.2°) and the C_{2v} monocapped trigonal prism (41.5, 0.0, and 0.0°).

The clustering of sulfur atoms in $[Ti(Et_2mtc)_3Cl]$ is in accord with previous structural studies,[3,35,36] which indicate that monothiocarbamate complexes tend to adopt structures that maximize the number of S···S contacts. The preferred stability of structures having an all-cis arrangement of sulfur atoms is not yet well understood, but it is relevant to observe that such structures are stabilized by a trans influence of the sulfur atoms.[3] The clustering of sulfur atoms cannot be accounted for by attractive S···S interactions, as has been demonstrated in the case of $[Ti(Et_2mtc)_4]$ and $[Zr(Et_2mtc)_4]$.[3] In $[Ti(Et_2mtc)_3Cl]$, only one S···S contact ($S_b \cdots S_c$, cf. Table VI) is shorter than twice the van der Waals radius of sulfur (1.72 Å[37]). For an easily deformed atom such as sulfur, however, such a short contact is not particularly unusual and is explainable in terms of crowding in the equatorial plane where all of the interligand contacts are shorter than the sum of the van der Waals radii. Crystal packing may also be ruled out as an explanation for the stability of the observed stereoisomer since $[Ti(Me_2mtc)_3Cl]$ exhibits the same stereochemistry in solution (vide infra).

Ti-Cl and Ti-S bond lengths in $[Ti(Et_2mtc)_3Cl]$ (Table VI) closely resemble those in the related dithiocarbamate complex, $[Ti(Me_2dtc)_3Cl]$.[33] The Ti-Cl distance of 2.330 (1) Å is slightly greater than that in the dithiocarbamate complex (2.305 (3) Å). The mean Ti-S distance of 2.481 Å is virtually identical with the mean length of the three Ti-S bonds in $[Ti(Me_2dtc)_3Cl]$ (2.482 Å) that point to the positions occupied by sulfur atoms in $[Ti(Et_2mtc)_3Cl]$; the averaged length of all six Ti-S bonds in $[Ti(Me_2dtc)_3Cl]$ (2.512 Å) is only slightly larger. Although it was expected that the axial Ti-S bond in $[Ti(Et_2mtc)_3Cl]$ might be shorter than the equatorial bonds, the lengths of the three Ti-S bonds are nearly equal. Interestingly, the mean Ti-S distance in $[Ti(Et_2mtc)_3Cl]$ is 0.09 Å less than that in $[Ti(Et_2mtc)_4]$ (2.571 Å),[3] suggesting that the Ti-S bonds in the seven-coordinate monothiocarbamate complex are somewhat stronger than those in the eight-coordinate analogue. The mean Ti-O bond length of 2.081 Å in $[Ti(Et_2mtc)_3Cl]$ is only 0.01 Å less than that in $[Ti(Et_2mtc)_4]$ (2.089 Å)[3], probably because the three oxygen atoms in $[Ti(Et_2mtc)_3Cl]$ lie in the crowded equatorial plane.

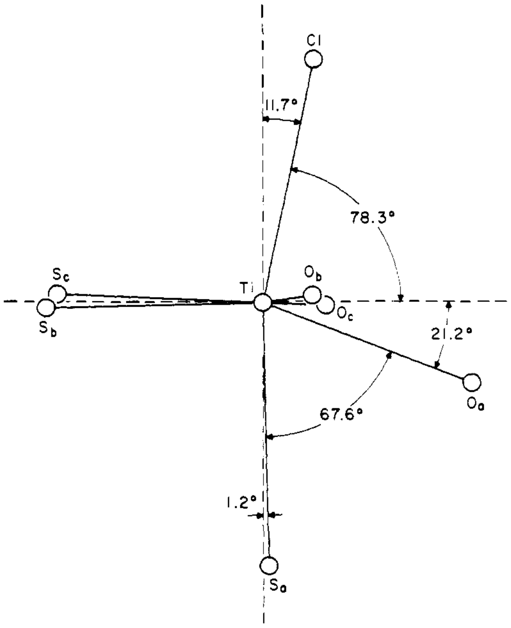

Figure 2. Projection of the TiS_3O_3Cl coordination group of $[Ti(Et_2mtc)_3Cl]$ on the quasi-mirror plane.

Bond lengths and angles within the monothiocarbamate ligands (Table VII) are consistent with the values reported for other monothiocarbamate complexes.[3,36] The dimensions of ligands b and c are essentially identical, but ligand a, which spans axial and equatorial positions, has a larger bite (by ~0.04 Å), a larger S-C-O angle (by 2.5°), and correspondingly smaller values of the C-S-Ti and C-O-Ti angles. These differences are probably related to the crowding of atoms in the equatorial plane of the coordination polyhedron, which forces the ligating atoms of ligands b and c closer together than the less hindered corresponding atoms of ligand a.

The six atoms of each $SOCNC_2$ monothiocarbamate skeleton are nearly coplanar, with the mean deviation of the 18 atoms of the three ligands from their respective mean planes being 0.033 Å; the maximum deviation is 0.080 Å (cf. Table VIII[32]). There is a slight (6.0°) twist about the C⩦N bond in ligand b. Ligand c is planar, as is ligand a, except for methylene carbon atom C_{a3}, which is displaced by 0.2 Å from the mean plane of the other five atoms of ligand a. The displacement of C_{a3} may arise from close nonbonded contacts involving the adjacent disordered carbon atom C_{a4}. There are five nonbonded contacts appreciably less than the sum of the van der Waals radii: $C_{a4a} \cdots C_{a4b}$ (3.59 Å), $C_{a4a} \cdots C_{b2}$ (3.62 Å), $C_{a4a} \cdots C_{c4}$ (3.74 Å), $C_{a4b} \cdots C_{c4}$ (3.75 Å), and $C_{c3} \cdots C_{c3}$ (3.71 Å). All but the last involve at least one of the sites of partial occupancy of C_{a4}. A packing diagram is shown in Figure 3. There is some folding of the chelate rings about the S···O edges of the coordination polyhedron; the dihedral angle between each ligand plane and the appropriate TiSO plane is 18.4, 11.5, and 0.8° for ligands a, b, and c, respectively.

Table VII. Bond Lengths (Å) and Bond Angles (deg) in the *N,N*-Diethylmonothiocarbamate Ligands[a]

bond	ligand a	ligand b	ligand c	av[b]	angle	ligand a	ligand b	ligand c	av[b]
S···O[c]	2.562 (3)	2.529 (3)	2.522 (3)	2.526 (3, 4, 4)[d]	S-C-O	116.1 (3)	114.2 (3)	113.0 (3)	113.6 (3, 6, 6)[d]
C-S	1.732 (5)	1.724 (4)	1.731 (4)	1.729 (4, 3, 5)	C-S-Ti	74.6 (1)	76.0 (1)	76.7 (1)	76.4 (1, 4, 4)[d]
C-O	1.274 (5)	1.272 (5)	1.278 (5)	1.275 (5, 2, 3)	C-O-Ti	99.4 (2)	102.1 (2)	103.9 (2)	103.0 (2, 9, 9)[d]
C-N	1.337 (5)	1.323 (5)	1.320 (5)	1.327 (5, 7, 10)	S-C-N	123.4 (4)	124.3 (3)	125.7 (3)	124.5 (3, 8, 12)
					O-C-N	120.5 (4)	121.4 (4)	121.3 (4)	121.1 (4, 4, 6)
C_1-N	1.484 (7)	1.482 (6)	1.479 (6)	1.485 (6, 8, 22)	C_1-N-C	121.4 (5)	122.0 (4)	122.6 (4)	122.0 (4, 4, 6)
C_3-N	1.507 (8)	1.480 (6)	1.475 (6)		C_3-N-C	118.9 (5)	120.1 (4)	119.0 (4)	119.3 (4, 5, 8)
					C_1-N-C_3	119.2 (4)	117.9 (4)	118.4 (4)	118.5 (4, 5, 7)
C_1-C_2	1.493 (9)	1.493 (9)	1.471 (9)	1.491 (9, 8, 20)[g]	N-C_1-C_2	114.3 (6)	111.6 (5)	112.7 (5)	112.7 (5, 8, 16)[g]
C_3-C_4	1.373 (13)[e] 1.277 (17)[f]	1.505 (8)	1.491 (10)		N-C_3-C_4	120.2 (9)[e] 116.5 (11)[f]	111.7 (4)	113.2 (5)	

[a] Numbers in parentheses are estimated standard deviations in the last significant figure. [b] The numbers in parentheses following each averaged value are the root mean square estimated standard deviation for an individual datum and the mean and maximum deviation from the average value. [c] The "bite" of the ligand. [d] Average for ligands b and c. [e] These data refer to the disordered carbon atom C_{a4a}. [f] These data refer to the disordered carbon atom C_{a4b}. [g] Distances and angles involving C_{a4a} and C_{a4b} are not included in the averages.

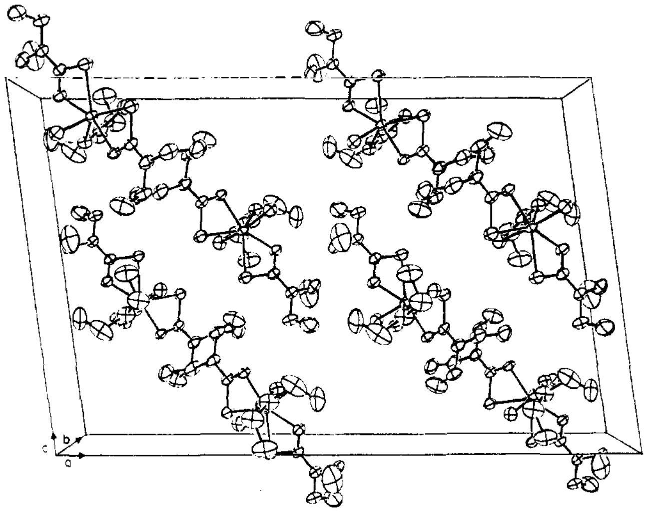

Figure 3. Model in perspective to illustrate the packing of [Ti(Et$_2$mtc)$_3$Cl] molecules in the crystal. The contents of one unit cell are viewed normal to the (010) plane.

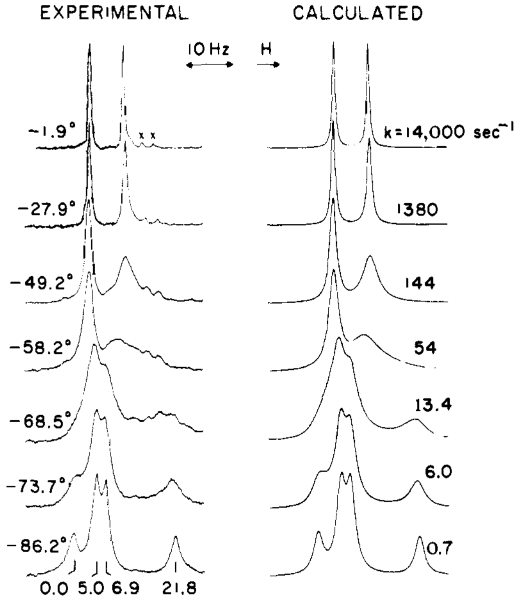

Figure 4. Observed and calculated line shapes for the methyl proton resonances of [Ti(Me$_2$mtc)$_3$Cl], 0.0590 M in CD$_2$Cl$_2$, at 90 MHz (low-temperature process). The peaks marked with an x are due to an impurity.

Stereochemistry and Rearrangement of [Ti(Me$_2$mtc)$_3$Cl] in Solution. ^{1}H NMR spectra of [Ti(Me$_2$mtc)$_3$Cl] at selected temperatures in the range −86 to −2 °C are presented in Figure 4. In the slow-exchange limit, this complex exhibits four methyl proton resonances of relative intensity 1:2:2:1, consistent with the pentagonal bipyramidal structure found in the solid state for [Ti(Et$_2$mtc)$_3$Cl]. The two low-field peaks and the two high-field peaks coalesce at approximately −58 °C to give a two-line pattern which sharpens with increasing temperature. To account for these line-shape changes, one must consider two possible kinetic processes: (1) metal-centered rearrangement and (2) hindered rotation about the C$\overset{\dots}{-}$N partial double bond in the planar monothiocarbamate ligands. Metal-centered rearrangement would destroy the inequivalence of the spanning ligand (ligand a in Figure 1) and the equatorial ligands (ligands b and c), thus collapsing the four methyl resonances into two time-averaged resonances of equal intensity. Rotation about the C$\overset{\dots}{-}$N bond would maintain the inequivalence of the spanning and equatorial ligands but would destroy the inequivalence arising from proximity to sulfur or oxygen; thus, two resonances of relative intensity 1:2 would be expected in the fast-exchange limit. Since the two resonances in the fast-exchange limit are equally intense (cf. Figure 4), the low-temperature kinetic process can be assigned unambiguously to metal-centered rearrangement.

At still higher temperatures, the two time-averaged methyl resonances coalesce to give a single time-averaged line owing to the onset of rapid C$\overset{\dots}{-}$N bond rotation; the coalescence temperature is approximately 110 °C for a diphenylmethane solution. Because of severe thermal decomposition at elevated temperatures, detailed line-shape analysis of the high-temperature process was not possible. However, a first-order rate constant of 18 s^{-1} at the coalescence temperature was estimated from the relation $k_c = \pi\delta\nu/\sqrt{2}$,[38] where $\delta\nu$ = 8.20 Hz is the frequency difference between the two resonances in the absence of exchange, extrapolated from lower temperatures to 110 °C. The corresponding free energy barrier to C$\overset{\dots}{-}$N bond rotation, $\Delta G^{\ddagger}$ (110 °C), is 20 kcal/mol.

A complete line-shape analysis was carried out for the low-temperature (metal-centered rearrangement) process using the procedure described in the Experimental Section. Theoretical spectra were calculated as a function of a single rate constant k since exchange of the spanning and equatorial ligands results in pairwise exchange of methyl groups ($k = k_{12} = k_{43} = 2k_{21} = 2k_{34}$, where 1, 2, 3, and 4 label the methyl environments associated with the four resonance lines in Figure

Table IX. Kinetic Data for Metal-Centered Rearrangement of $[Ti(Me_2mtc)_3Cl]$[a]

temp, °C	T_2, s[b]	chemical shifts, Hz[c] 2	3	4	k, s^{-1}
−86.2	0.145	4.95	7.00	21.75	0.7
−79.8	0.159	5.07	7.02	21.65	2.00
−76.9	0.166	5.12	7.03	21.60	3.91
−73.7	0.174	5.18	7.03	21.54	6.0
−71.6	0.180	5.22	7.04	21.51	8.8
−68.5	0.188	5.27	7.04	21.45	13.4
−66.1	0.195	5.32	7.05	21.42	18.6
−63.9	0.202	5.36	7.05	21.38	26.2
−58.2	0.220	5.46	7.06	21.28	54
−55.1	0.231	5.52	7.06	21.23	68
−53.0	0.238	5.55	7.07	21.19	86
−49.2	0.252	5.63	7.09	21.13	144
−45.3	0.267	5.70	7.10	21.07	186
−40.8	0.286	5.78	7.10	20.99	410
−34.4	0.314	5.89	7.12	20.89	730
−27.9	0.347	6.01	7.13	20.77	1380

Activation Parameters

E_a, kcal/mol	11.6 ± 0.3	T_c,[d] °C	−58.2
log A	13.5 ± 0.3	$\Delta G^{\ddagger}(T_c)$, kcal/mol	10.78 ± 0.10
$\Delta H^{\ddagger}$, kcal/mol	11.2 ± 0.3	$\Delta G^{\ddagger}$(25 °C), kcal/mol	10.62 ± 0.14
$\Delta S^{\ddagger}$, eu	2.0 ± 1.6	k(25 °C), s^{-1}	9.8×10^4

[a] 0.0590 M in CD_2Cl_2. The uncertainties in the activation parameters are random errors estimated at the 95% confidence level. [b] Transverse relaxation time. [c] Chemical shifts of the three lines at higher field, in order of increasing field, relative to the line at lowest field. [d] Approximate coalescence temperature.

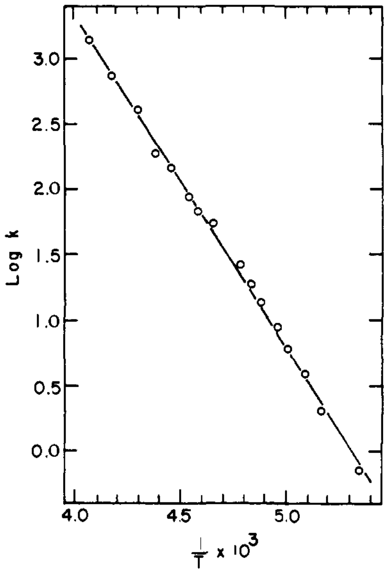

Figure 5. Arrhenius plot for the low-temperature exchange process in $[Ti(Me_2mtc)_3Cl]$.

4, in order of increasing field). Chemical shifts were also varied in the calculation of theoretical spectra, with the constraint that chemical shifts be a linear function of temperature. Values of T_2, chemical shifts, and k required for best agreement between observed and calculated spectra are listed in Table IX. Also presented in Table IX are Arrhenius and Eyring activation parameters and the extrapolated value of k at 25 °C; the Arrhenius and Eyring parameters were obtained in the usual way from the least-squares straight lines of a log k vs. $1/T$ plot (Figure 5) and a log (k/T) vs. $1/T$ plot, respectively. The agreement between experimental and calculated spectra is illustrated in Figure 4.

An intramolecular mechanism for metal-centered rearrangement of $[Ti(Me_2mtc)_3Cl]$ is established by the following experimental evidence. First, rate constants for 0.0271 and 0.0590 M solutions are equal within experimental error, indicating that the rearrangement is first order in $[Ti(Me_2mtc)_3Cl]$. Second, the ^1H NMR spectrum at 34 °C of a dichloromethane solution containing both $[Ti(Me_2mtc)_3Cl]$ and $[Ti(Me_2mtc)_3Br]$ showed separate resonances for each complex, indicating that halide exchange is slow on the NMR time scale at temperatures 90 °C above the coalescence temperature (−58 °C) for metal-centered rearrangement; this experiment demonstrates that metal-centered rearrangement does not involve complete dissociation of the halide ion. Third, ^1H NMR spectra of $[Ti(Me_2mtc)_3Cl]$ in dichloromethane solution exhibit two methyl resonances from −58 (Figure 4) to +74 °C, consistent with the fact that $C \overset{\dots}{-} N$ bond rotation is slow on the NMR time scale in this temperature range. Since $C \overset{\dots}{-} N$ bond rotation in the $(Me_2mtc)^-$ anion is fast on the NMR time scale at 34 °C, complete dissociation of monothiocarbamate ligands from $[Ti(Me_2mtc)_3Cl]$ must be slow on the NMR time scale at 34–74 °C. Therefore, metal-centered rearrangement cannot involve complete dissociation of monothiocarbamate ligands.

The possible intramolecular rearrangement mechanisms are of two types: (1) "arm-on, arm-off" mechanisms that involve opening of a chelate ring to give a six-coordinate intermediate and (2) polytopal rearrangement mechanisms that effect exchange of spanning and equatorial ligands without metal-ligand bond rupture. An attractive polytopal rearrangement is depicted in Figure 6; the postulated transition state has a monocapped octahedral coordination polyhedron with the chlorine atom in the capping site and the three sulfur atoms in cis positions on the opposite triangular face. Since the transition state has C_3 symmetry, the distinction between spanning and equatorial ligands is lost, and ligand exchange is effected when the complex returns to pentagonal bipyramidal geometry. An obvious advantage of this mechanism is that it maintains the characteristic all-cis arrangement of sulfur atoms throughout the rearrangement.

We prefer polytopal rearrangement over a ring-opening mechanism because of a substantial difference in the rates of rearrangement of $[Ti(Me_2mtc)_3Cl]$ and $[Ti(Me_2dtc)_3Cl]$; the dithiocarbamate complex is nonrigid on the NMR time scale,

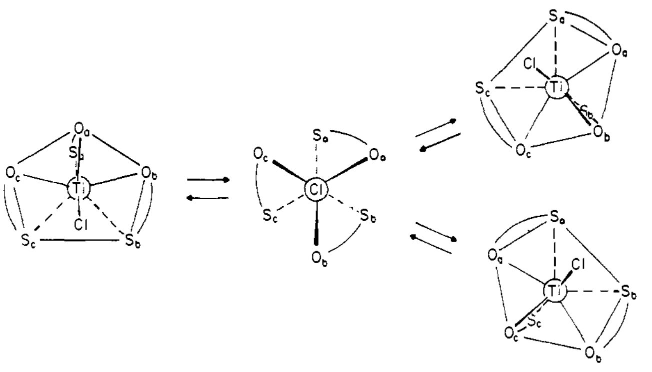

Figure 6. Exchange of methyl groups in $[\mathrm{Ti(Me_2mtc)_3Cl}]$ via a polytopal rearrangement involving a monocapped octahedral transition state of C_3 symmetry. The pentagonal bipyramids and the capped octahedron are viewed normal to the triangular face defined by the three sulfur atoms.

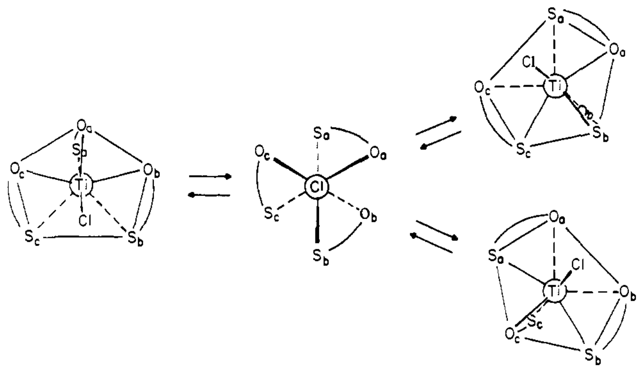

Figure 7. Alternate polytopal rearrangement mechanism for $[\mathrm{Ti(Me_2mtc)_3Cl}]$ involving a monocapped octahedral transition state of C_1 symmetry. The perspective is the same as in Figure 6.

even at −90 °C.[10] Since the Ti–S bond lengths in the closely related monothio- and dithiocarbamate complexes $[\mathrm{Ti(Et_2mtc)_3Cl}]$ and $[\mathrm{Ti(Me_2dtc)_3Cl}]$ are nearly equal (vide supra), the difference in rearrangement rates is not expected if the mechanism involves Ti–S bond rupture. Moreover, Ti–S bond rupture by itself does not effect exchange of spanning and equatorial ligands; it would have to be followed by polytopal rearrangement in the six-coordinate intermediate. Polytopal rearrangement in the seven-coordinate complex is much more likely.[39]

The greater rigidity of $[\mathrm{Ti(Me_2mtc)_3Cl}]$ relative to the dithiocarbamate analogue can be rationalized in terms of the presumed tendency of the sulfur atoms to maintain an all-cis configuration throughout the rearrangement. This severely limits the number of allowed rearrangement pathways for the monothiocarbamate. For example, the alternate polytopal rearrangement shown in Figure 7 would not be allowed for the monothiocarbamate because the monocapped octahedral transition state does not have an all-cis arrangement of sulfur atoms. Note also that the rearrangement in Figure 7 leads to geometric isomerization, and more than one step would be required to exchange spanning and equatorial ligands in the observed stereoisomer. The rearrangement in Figure 7, is, however, an acceptable pathway for exchange of inequivalent methyl groups in the dithiocarbamate analogue $[\mathrm{TiMe_2dtc)_3Cl}]$ where all of the chelating donor atoms are sulfur atoms. Indeed, from a steric point of view, one could argue that the motion in Figure 7 is preferred over that in Figure 6. In Figure 7, the three atoms Cl, O$_b$, and S$_b$ undergo a concerted clockwise rotational motion on going to the monocapped octahedral transition state, whereas in Figure 6 a similar motion of the Cl atom but a counterclockwise digonal twisting of ligand b result in an unfavorable steric interaction between the atoms Cl and O$_b$. Such an interaction may raise the energy barrier for the polytopal rearrangement in Figure 6, thus accounting for the unusual rigidity of $[\mathrm{Ti(Me_2mtc)_3Cl}]$. So far as we know, this complex is only the second seven-coordinate halotris(chelate) that has been reported to be stereochemically rigid on the NMR time scale.[7]

The general point that emerges from the discussion in the preceding paragraph is that low-energy paths for polytopal rearrangement of higher coordination complexes may be inaccessible in complexes that contain unsymmetrical chelating ligands because of strong donor atom site preferences in the transition state. Rearrangement must then proceed by a higher energy pathway. It appears, therefore, that studies of unsymmetrical chelates may be a most fertile area of investigation in future searches for stereochemical rigidity in higher coordination complexes. An example of the importance of donor atom site preferences in slowing the rearrangement of an eight-coordinate chelate has been reported by Archer and Donahue.[5]

Acknowledgments. The support of this research by National Science Foundation Grant CHE-7620300 is gratefully acknowledged. We thank Professors J. L. Hoard and R. E. Hughes for access to the diffractometer, Drs. W. L. Steffen and H. K. Chun for assistance with the crystallographic study, and Mr. M. F. Wheeler for the synthesis and characterization of $[\mathrm{Ti(Me_2mtc)_3Br}]$.

Supplementary Material Available: A listing of structure factor amplitudes for $[\mathrm{Ti(Et_2mtc)_3Cl}]$ and Table VIII, least-squares mean planes and atomic displacements from these planes for $[\mathrm{Ti(Et_2mtc)_3Cl}]$ (24 pages). Ordering information is given on any current masthead page.

References and Notes

(1) W. L. Steffen, S. L. Hawthorne, and R. C. Fay, *J. Am. Chem. Soc.*, **98**, 6757 (1976).
(2) S. L. Hawthorne, A. H. Bruder, and R. C. Fay, *Inorg. Chem.*, **17**, 2114 (1978).
(3) W. L. Steffen and R. C. Fay, *Inorg. Chem.*, **17**, 2120 (1978).
(4) (a) R. C. Fay, D. F. Lewis, and J. R. Weir, *J. Am. Chem. Soc.*, **97**, 7179 (1975); (b) D. F. Lewis and R. C. Fay, *Inorg. Chem.*, **15**, 2219 (1976).
(5) (a) R. D. Archer and C. J. Donahue, *J. Am. Chem. Soc.*, **99**, 269 (1977); (b) C. J. Donahue and R. D. Archer, *ibid.*, **99**, 6613 (1977).
(6) (a) R. C. Fay and J. K. Howie, *J. Am. Chem. Soc.*, **99**, 8110 (1977); (b) *ibid.*, **101**, 1115 (1979).
(7) Miessler and Pignolet[8] have very recently reported that $\mathrm{Ru(S_2CNMe_2)_2(\eta^2\text{-}SCNMe_2)Cl}$ is rigid at −40 °C. The following complexes of the type M(chelate)$_3$X are nonrigid on the NMR time scale, even at low temperatures: Zr(acac)$_3$Cl,[9] Zr(acac)$_3$Br,[9] Ti(R$_2$dtc)$_3$Cl (R$_2$dtc = *N,N*-dialkyldithiocarbamate; R = Me, Et, or *i*-Bu),[10] Ru(Et$_2$dtc)$_3$Cl,[11] Ru(R$_2$dtc)$_3$I·I$_2$ (R = Me, Et, or Bzl).[11b,12] In contrast, analogous $(\eta^5\text{-}\mathrm{C_5H_5})\mathrm{Zr}(\beta\text{-diketonate})_3$,[13] $(\eta^5\text{-}\mathrm{C_5H_5})\mathrm{M(Me_2dtc)_3}$ (M = Ti,[14,15] Zr,[15-17] or Hf[15]), Mo(NO)(Me$_2$dtc)$_3$,[18] and Mo(NS)(Me$_2$dtc)$_3$[19] complexes are stereochemically rigid on the NMR time scale at readily accessible temperatures. Indeed, most of these complexes are rigid at room temperature.
(8) G. L. Miessler and L. H. Pignolet, *Inorg. Chem.*, **18**, 210 (1979).
(9) T. J. Pinnavaia and R. C. Fay, *Inorg. Chem.*, 7, 502 (1968).
(10) A. N. Bhat, R. C. Fay, D. F. Lewis, A. F. Lindmark, and S. H. Strauss, *Inorg. Chem.*, **13**, 886 (1974).
(11) (a) K. W. Given, B. M. Mattson, and L. H. Pignolet, *Inorg. Chem.*, **15**, 3152 (1976); (b) S. H. Wheeler, B. M. Mattson, G. L. Miessler, and L. H. Pignolet, *ibid.*, **17**, 340 (1978).
(12) B. M. Mattson and L. H. Pignolet, *Inorg. Chem.*, **16**, 488 (1977).
(13) (a) M. Elder, J. G. Evans, and W. A. G. Graham, *J. Am. Chem. Soc.*, **91**, 1245 (1969); (b) J. J. Howe and T. J. Pinnavaia, *ibid.*, **92**, 7342 (1970); (c) T. J. Pinnavaia, J. J. Howe, and R. E. Teets, *Inorg. Chem.*, **13**, 1074 (1974).
(14) W. L. Steffen, H. K. Chun, and R. C. Fay, *Inorg. Chem.*, **17**, 3498 (1978).
(15) J. R. Weir, A. H. Bruder, and R. C. Fay, to be submitted for publication.
(16) A. H. Bruder, R. C. Fay, D. F. Lewis, and A. A. Sayler, *J. Am. Chem. Soc.*, **98**, 6932 (1976).
(17) V. K. Jain, B. S. Garg, and R. P. Singh, *Aust. J. Chem.*, **30**, 2545 (1977).
(18) (a) B. F. G. Johnson, J. A. McCleverty, and K. H. Al-Obaidi, *J. Chem. Soc. A*, 1668 (1969); (b) R. Davis, M. N. S. Hill, C. E. Holloway, B. F. G. Johnson, and K. H. Al-Obaidi, *ibid.*, 994 (1971).
(19) J. Chatt and J. R. Dilworth, *J. Chem. Soc., Chem. Commun.*, 508 (1974).
(20) A. L. Van Geet, *Anal. Chem.*, **42**, 679 (1970).
(21) A. Allerhand, H. S. Gutowsky, J. Jonas, and R. A. Meinzer, *J. Am. Chem. Soc.*, **88**, 3185 (1966).
(22) R. W. Jones, Jr., and R. C. Fay, *Inorg. Chem.*, **12**, 2599 (1973).
(23) (a) R. L. Middaugh, R. S. Drago, and R. J. Niedzielski, *J. Am. Chem. Soc.*,

86, 388 (1964); (b) A. E. Lemire and J. C. Thompson, *Can. J. Chem.*, **48**, 824 (1970).
(24) A. H. Bruder, S. L. Hawthorne, and R. C. Fay, to be submitted for publication.
(25) N. F. M. Henry and K. Lonsdale, Eds., "International Tables for X-ray Crystallography", Vol. 1, 3rd ed., Kynoch Press, Birmingham, England, 1969, p 101.
(26) E. R. Howells, D. C. Phillips, and D. Rogers, *Acta Crystallogr.*, **3**, 210 (1950).
(27) L. J. Radonovich, A. Bloom, and J. L. Hoard, *J. Am. Chem. Soc.*, **94**, 2073 (1972).
(28) D. T. Cromer and J. B. Mann, *Acta Crystallogr., Sect. A*, **24**, 321 (1968).
(29) R. F. Stewart, E. R. Davidson, and W. T. Simpson, *J. Chem. Phys.*, **42**, 3175 (1965).
(30) D. T. Cromer, *Acta Crystallogr., Sect. A*, **18**, 17 (1965).
(31) B. J. McCormick and B. P. Stormer, *Inorg. Chem.*, **11**, 729 (1972).
(32) See paragraph at end of paper regarding supplementary material.
(33) D. F. Lewis and R. C. Fay, *J. Am. Chem. Soc.*, **96**, 3843 (1974).
(34) E. L. Muetterties and L. J. Guggenberger, *J. Am. Chem. Soc.*, **96**, 1748 (1974). See also the erratum: *ibid.*, **99**, 3893 (1977).
(35) J. Ahmed and J. A. Ibers, *Inorg. Chem.*, **16**, 935 (1977).
(36) C. G. Pierpont, R. C. Dickinson, and B. J. McCormick, *Inorg. Chem.*, **13**, 1674 (1974).
(37) D. van der Helm, A. E. Lessor, Jr., and L. L. Merritt, Jr., *Acta Crystallogr.*, **15**, 1227 (1962).
(38) H. S. Gutowsky and C. H. Holm, *J. Chem. Phys.*, **25**, 1228 (1956).
(39) E. L. Muetterties, *Acc. Chem. Res.*, **3**, 266 (1970).

Olefin Formation from Platinacyclobutanes

Thomas H. Johnson* and Sheng-San Cheng

Contribution from the Department of Chemistry, Kansas State University, Manhattan, Kansas 66506. *Received February 7, 1979*

Abstract: Deuterium-labeled cyclopropanes **6a–c** were synthesized and reacted with Zeise's dimer to give the platinacyclobutanes **7a–c**. Decomposition of these platinacyclobutanes gave deuterium-labeled 2,3-dimethylbut-1-enes **8–13**. The results indicated that the olefins were formed from what is formally a β-hydrogen abstraction followed by a reductive elimination. The results also indicated that an α-hydrogen abstraction process was not operative. Two types of β-hydrogen abstraction processes were possible and both occurred, although β-hydrogen abstraction from the ring of the platinacylobutane was favored over β-hydrogen abstraction from a methyl substituent. The dissociated pyridine did not participate in the hydrogen-abstraction process. Additionally, the rearrangement of **4** to **1** was shown not to occur by a 1,2-methyl migration which had been previously suggested as a possible rearrangement route.

Zeise's dimer[1] reacts with cyclopropanes to form platinacyclobutanes.[2,3] Phenylcyclopropane forms a platinacyclobutane which undergoes interesting rearrangement reactions[4] and has been the subject of mechanistic inquiries.[5] Conversely, the chemistry of platinacyclobutanes formed from alkyl-substituted cyclopropanes is dominated by olefin formation.[3] Olefin formation has also been reported to be a dominant pathway in the decomposition of platinacyclopentanes.[6] Both aryl- and alkyl-substituted platinacyclobutanes will give cyclopropanes upon treatment with phosphines or aqueous KCN[2,3] and there has been a rearrangement observed for one alkyl-substituted platinacyclobutane.[7] In this paper we report upon a study of olefin formation from dichlorobis(pyridine)-(1,1,2-trimethylpropane-1,3-diyl)platinum(IV) (**1**).

Results

Complex **1** was prepared according to the method of Brown[7] and was decomposed in $CHCl_3$ at 25 ± 2 °C to give 2,3-dimethylbut-1-ene as the major product (>95%). The olefin **2** could in theory arise by at least three independent routes from **1** as illustrated in Scheme I.

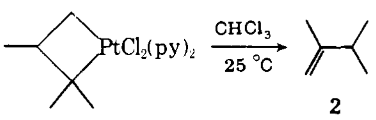

1 **2**

The three routes all require prior dissociation of a pyridine ligand, a process which has been established in platinacyclobutane chemistry.[4,5] Olefin formation routes (b) and (c) require the well-known β-hydrogen abstraction (β-hydride elimination) reaction followed by the equally well-known reductive elimination process.[8] Route (a) requires an α-hydrogen abstraction prior to reductive elimination.[8] Whitesides found that methyl-substituted platinacyclopentanes failed to form olefins significantly faster than their unsubstituted analogues.[6]

Scheme I

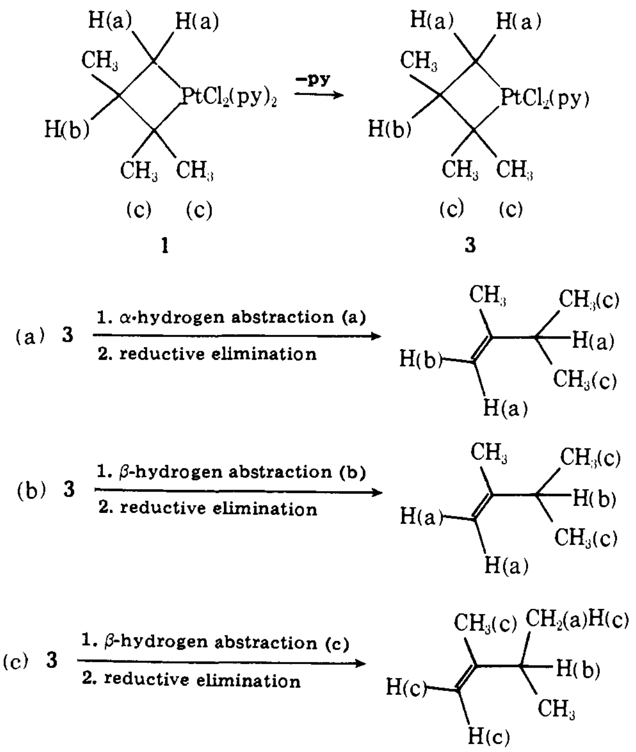

By the preparation of deuterium-labeled cyclopropanes we hoped to differentiate between the three possible modes of olefin formation and to gain some insight into reactivity differences between a ring-substituted β hydrogen vs. the β hydrogen of a methyl substituent.

Additionally, Brown has shown that **1** is the rearranged product of dichlorobis(pyridine)(1,2,2-trimethylpropane-

0002-7863/79/1501-5277$01.00/0